Image Cover Sheet

98-00047

CLASSIFICATION	SYSTEM NUMBER
UNCLASSIFIED	506552

TITLE

AN EFFICIENT PIECEWISE MATCHED-FIELD TRACKING ALGORITHM

System Number:

Patron Number:

Requester:

Notes:

DSIS Use only:

Deliver to:

An efficient piecewise matched-field tracking algorithm

MICHAEL J. WILMUT
Dept. of Mathematics and Computer Science, Royal Military College,
PO BOX 17000 STN FORCES, Kingston, ON, K7K 7B4

JOHN M. OZARD and KYLE O'KEEFE
Esquimalt Defence Research Detachment, Defence Research Establishment Atlantic,
PO BOX 17000 STN FORCES, Victoria, BC, V9A 7N2

MARTIN MUSIL
School of Earth and Ocean Sciences, University of Victoria, Victoria, BC, V8W 2Y2

Abstract

Efficient matched-field tracking (MFT) algorithms have been successfully applied to both simulated and measured data to determine the most likely positions of a sound source that is localized ambiguously by a matched-field processing (MFP) system. They have been used to track sources moving linearly or on a circular path at constant speed and heading. The input to the trackers is a set of ambiguity surfaces, contiguous in time, generated by MFP. These algorithms assume that the track start and end times are known *a priori*; this restriction is removed in the Piecewise MFT algorithm (PTA). In a series of simulations it is shown that the statistically significant tracks, including their unknown start and end times, can be found with a mean absolute error equal to the time covered by 3 or fewer ambiguity surfaces, depending on the propagation and provided the track signal-to-noise ratio is greater than 13. The PTA was applied to measured data collected during the PACIFIC SHELF 93 trial to successfully identify the significant source track segments.

1 Introduction

Matched-Field Processing (MFP) matches a measured acoustic field with a predicted field, based on a model of the environment and a propagation model, for all possible locations of an acoustic source in a search region [1]. In this study, matching is conducted with a Bartlett beamformer and the result is an ambiguity surface consisting of Bartlett statistics, $B(\mathbf{r})$, representing the likelihood that the source is present at any position in the search region. If MFP is repeated for data collected over a length of time, the result is a series of ambiguity surfaces. It is then possible to track the movement of probable sources over time.

Linear and circular trackers [2, 3, 4] determine candidate source tracks that pass through a series of ambiguity surfaces by connecting the top two or three peaks on different surfaces by lines or circles respectively. They are limited however in that they report linear or

circular tracks through the entire series of ambiguity surfaces when in fact the source may only be present at a sufficiently high signal level along a particular line or circle in some of the ambiguity surfaces. This paper presents an efficient piecewise matched-field tracking algorithm (PTA) for finding the portion of a track that maximizes the track signal-to-noise ratio (SNR). Thus start and stop points of significant track segments can be found within a series of ambiguity surfaces so that it becomes possible to track a source that changes course or becomes quiet during the time of observation. The performance of the PTA is given for some simulated cases of interest and the PTA is applied to measured data from the PACIFIC SHELF sea trial previously analyzed using the linear tracking algorithm [5].

2 Efficient Tracking Algorithms

Previously-developed linear and circular trackers consist of five sets of computations, the first three of which are the same for both the unweighted algorithm and the weighted algorithm [3]. The computations are:

(1) for each of the N_s surfaces the positions of the largest N_{pk} peaks are determined;

(2) all possible linear tracks joining two peaks on different surfaces are found. These are called combinatoric tracks.

(3) a constraint to realistic maximum speeds for the target is imposed to reduce the combinatoric tracks to the physically possible tracks.

For uniform weighting, which is hereafter called unweighted, the last two computations are:

(4a) the unweighted track statistic, T_u, is calculated for each physically possible track:

$$T_u = \frac{1}{N_s} \sum_{k=1}^{N_s} B(\mathbf{r}_k) \tag{1}$$

where $B(\mathbf{r}_k)$ is the normalized Bartlett output for the replica vector $\mathbf{r}_k$ on the k^{th} surface along track.

(5a) the estimated unweighted track signal-to-noise ratio (SNR) outputs, $\widehat{SNR}_u$ are calculated:

$$\widehat{SNR}_u = \frac{T_u - \overline{x}}{s} \sqrt{N_s} \tag{2}$$

where $\overline{x}$ and s are the average value and standard deviation of the Bartlett statistic in noise alone. These can be estimated by calculating the mean and standard deviation

of the Bartlett statistics at a neighbouring frequency in the same search region. The quantity $\widehat{SNR}_u$ is the difference between the unweighted track statistic and the mean level of the Bartlett statistic of the noise measured in multiples of the standard deviation of the Bartlett statistic of the noise. It is a measure of the statistical significance of the track: the larger this quantity is, the more unlikely it is that the associated track represents noise.

For propagation weighting, hereafter called weighted, the last two computations are:

(4b) the weighted track statistic, T_w, is calculated for each physically possible track:

$$T_w = \sum_{k=1}^{N_s} c_k B(\mathbf{r}_k) \tag{3}$$

where c_k is the Bartlett output (signal only) at the k^{th} point along the track normalized over the N_s points in the track:

$$c_k = \frac{\lambda_k}{\sum_{k=1}^{N_s} \lambda_k} \tag{4}$$

where λ_k is the theoretical unnormalized Bartlett output (signal only) for the k^{th} surface. (Note that for uniform weighting, $c_k = \frac{1}{N_s}$.) It is important from a practical point of view to recognize that the modeled signal powers may be scaled by a constant without affecting the values of c_k in the algorithm or the algorithm output.

(5b) the estimated weighted track SNR outputs, $\widehat{SNR}_w$ are calculated:

$$\widehat{SNR}_w = \frac{T_w - \overline{x}}{s\sqrt{\sum_{k=1}^{N_s} c_k^2}}. \tag{5}$$

Circular tracking is accomplished with a modification to steps 2 and 3 of the linear tracking algorithm. Instead of finding linear tracks though two peaks on different surfaces, circular tracks through three peaks on different surfaces are found. The physically possible tracks are then determined by limiting the speed and the radius of the track.

3 Identifying significant track segments

Piecewise tracking adds the determination of the most significant sections of the tracks found in the first three steps of the linear and circular algorithms. This removes the need to know the start and stop surfaces of the tracks *a priori* and is done by finding the portion of the track that maximizes $\widehat{SNR}_u$ or $\widehat{SNR}_w$.

To simplify the the piecewise algorithm, the estimated mean noise level of the Bartlett statistics, $\overline{x}$, is subtracted from the Bartlett statistics. If $B'(\mathbf{r}_k)$ is defined as $B(\mathbf{r}_k) - \overline{x}$, then let

$$T'_u = \frac{1}{N_s} \sum_{k=1}^{N_s} B'(\mathbf{r}_k) \tag{6}$$

and equation (2) becomes,

$$\widehat{SNR}_u = \frac{T'_u}{s} \sqrt{N_s}. \tag{7}$$

Combining the two leads to:

$$\widehat{SNR}_u = \frac{1}{s\sqrt{N_s}} \sum_{k=1}^{N_s} B'(\mathbf{r}_k). \tag{8}$$

Similarly, for the weighted case, let

$$T'_w = \sum_{k=1}^{N_s} c_k B'(\mathbf{r}_k) \tag{9}$$

and equation (5) becomes,

$$\widehat{SNR}_w = \frac{T'_w}{s\sqrt{\sum_{k=1}^{N_s} c_k^2}}. \tag{10}$$

Combining these two leads to:

$$\widehat{SNR}_w = \frac{1}{s\sqrt{\sum_{k=1}^{N_s} c_k^2}} \sum_{k=1}^{N_s} c_k B'(\mathbf{r}_k). \tag{11}$$

The most significant section of a track is then determined by finding I and J where $1 \leq I \leq J \leq N_s$ such that the unweighted or weighted track SNR on surfaces I through J is maximized. The unweighted track SNR, denoted $\widehat{SNR}_{pu}$, is given by

$$\widehat{SNR}_{pu} = \max_{\substack{1 \leq I \leq i \\ j \leq J \leq N_s}} \frac{1}{s\sqrt{J-(I-1)}} \sum_{k=I}^{J} B'(\mathbf{r}_k) \tag{12}$$

where i and j are the two peaks used to form the candidate linear track or the two outer peaks of the three peaks used to form the candidate circular track, and I and J are the start and stop points of the significant track.

For the propagation weighted case, with weights c_k, the weighted track SNR on surfaces I through J, $\widehat{SNR}_{pw}$, is

$$\widehat{SNR}_{pw} = \max_{\substack{1 \leq I \leq i \\ j \leq J \leq N_s}} \frac{1}{s\sqrt{\sum_{k=I}^{J} c_k^2}} \sum_{k=I}^{J} c_k B'(\mathbf{r}_k). \tag{13}$$

4 PTA Performance on simulated data

An indication of the piecewise tracking algorithm's performance was obtained using simulated data. Simulated time series of Bartlett statistics, $B(\mathbf{r}_k)$ were generated, along a straight line path containing noise only and signal plus noise segments. Only the values in the ambiguity surfaces on the track were simulated. Performance is defined as the accuracy to which the start and end surfaces of the track are found as a function of the track signal-to-noise ratio, track and time series length, and the number of averages used to form the Bartlett statistics.

More precisely, the received narrowband frequency data in the Bartlett statistics is the sum of noise plus signal, if present. The noise is assumed to be spatially white with Gaussian amplitude and the signal a constant with unknown uniformly distributed phase. These are idealized assumptions often used to model many environments [1, 3] and ones amenable to analysis.

For the above assumptions, the Bartlett noise statistics are chi-squared random variables with $2n$ degrees of freedom where n is the number of time snapshots used to form the Bartlett statistic. Likewise, a Bartlett statistic containing signal is a non-central chi-squared random variable with non-central parameter λ and $2n$ degrees of freedom where λ represents the mean signal strength.

The piecewise tracking algorithm was first tested on the simulated Bartlett time series whose length corresponds to 80 ambiguity surfaces. The signal was present on N surfaces. Each surface represents one independent time snapshot, so $n = 1$. Runs were conducted for all even values of N from 6 to 40 and values of λ from 0 to 10 in steps of 0.2. Propagation effects were simulated by making the signal strength a normal random variable with mean λ and standard deviation σ_w. The signal duration was uniformly distributed between 1 and 6 time segments The randomly generated signal strength, λ, served both as the non-central parameter for the chi-squared distributed time series and as the weights, c_k, that were provided to the weighted algorithm. Values of σ_w from 0 to 1.2 in steps of 0.4 were used. These values of the standard deviation of the signal strength, σ_w, as well as the random durations, were chosen to generate random propagation effects similar to those studied in a previous paper [3] and typical of an Arctic shallow water environment. These were also similar to the theoretical signal strength along radial tracks in the PACIFIC SHELF environment studied in section 5.

The simulations then consisted of applying linear unweighted and weighted piecewise tracking algorithms more than 1000 times to simulated data generated for each combination of N, λ and σ_w. (The position of the signal in the series was varied during each run so that each possible position of the signal occurred an equal number of times.)

The effectiveness of the algorithm was measured by calculating the mean absolute error

between the signal's true and estimated start and end points. The mean absolute error as a function of λ and N for $\sigma_w = 0.8$ are shown as contour plots in Figures 1 and 2 for the unweighted and weighted cases respectively when one snapshot is used to form the Bartlett statistics.

Since the simulated test data contains noise with standard deviation 2 and square pulses of mean amplitude λ and width N, $\frac{\lambda}{2}\sqrt{N}$ is the input track *SNR*. It is reasonable to assume the PTA's performance depends approximately on the track *SNR* and indeed the contours in Figures 1 and 2 do approximate contours of constant $\frac{\lambda}{2}\sqrt{N}$. Table 1 summarizes the effectiveness of both forms of the algorithm as a function of *SNR* ($\frac{\lambda}{2}\sqrt{N}$) and σ_w for Bartlett statistics obtained from a single snapshot.

Table 1: Average mean absolute error in locating endpoints for various *SNR*'s when signals have a non-central χ^2 distribution with 2 degrees of freedom and are found in a series of length 80. The *SNR* is in linear units.

SNR	Average estimated mean absolute errors for various σ_w and *SNR* ranges.							
	$\sigma_w = 0.0$		$\sigma_w = 0.4$		$\sigma_w = 0.8$		$\sigma_w = 1.2$	
range	weighted	uniform	weighted	uniform	weighted	uniform	weighted	uniform
1–3	13.48 ± 0.29	13.53	13.39	13.42	13.26	13.39	13.03	13.30
3–5	8.090 ± 0.154	8.059	8.153	8.102	8.387	8.225	8.547	8.300
5–7	4.896 ± 0.115	4.846	5.171	4.948	5.589	5.364	5.949	5.743
7–9	3.049 ± 0.102	3.037	3.388	3.252	3.928	3.735	4.330	4.325
9–11	2.082 ± 0.090	2.099	2.335	2.305	2.895	2.872	3.354	3.584
11–13	1.507 ± 0.072	1.527	1.684	1.716	2.119	2.361	2.572	3.134
13–15	1.187 ± 0.052	1.188	1.294	1.421	1.590	2.122	1.983	2.937
15–17	0.981 ± 0.040	0.992	1.050	1.229	1.286	1.987	1.576	2.907
17–19	0.825 ± 0.031	0.811	0.876	1.072	1.074	1.883	1.355	2.885
19–21	0.720 ± 0.022	0.710	0.764	0.955	0.949	1.822	1.199	2.898

This procedure was then repeated using chi-squared random variables with 8 degrees of freedom to simulate Bartlett statistics obtained by averaging 4 time snapshots. The results of these simulations are shown in Table 2.

Use of the weighted form of the algorithm did cause an interesting effect: The weighted algorithm gives consistently larger errors for low *SNR*. It was found that though propagation weighting resulted in slightly better performance for longer length signals, it caused larger errors to occur for shorter and lower amplitude signals. This effect can be seen by examination of Tables 1 and 2.

This result can be explained by the fact that the weighted algorithm, though derived from the LTA in exactly the same way as the uniform algorithm, assumes too much. Since

Table 2: Average mean absolute error in locating endpoints for various *SNR*'s when signals have a non-central χ^2 distribution with 8 degrees of freedom and are found in a series of length 80. The *SNR* is in linear units.

SNR range	Average estimated mean absolute errors for various σ_w and *SNR* ranges.							
	$\sigma_w = 0.0$		$\sigma_w = 0.8$		$\sigma_w = 1.6$		$\sigma_w = 2.4$	
	weighted	uniform	weighted	uniform	weighted	uniform	weighted	uniform
1–3	13.99 ± 0.33	13.99	14.03	13.93	14.01	13.91	13.77	13.78
3–5	7.701 ± 0.188	7.642	7.891	7.705	8.170	7.913	8.257	7.959
5–7	3.727 ± 0.102	3.723	4.185	3.924	4.821	4.410	5.079	4.908
7–9	1.736 ± 0.067	1.739	2.120	2.017	2.818	2.693	3.363	3.513
9–11	0.955 ± 0.049	0.945	1.229	1.205	1.863	1.925	2.485	2.836
11–13	0.616 ± 0.034	0.620	0.777	0.821	1.248	1.526	1.826	2.483
13–15	0.467 ± 0.026	0.471	0.551	0.667	0.842	1.382	1.269	2.336
15–17	0.388 ± 0.020	0.383	0.430	0.565	0.642	1.309	0.965	2.334
17–19	0.319 ± 0.017	0.323	0.358	0.493	0.522	1.239	0.796	2.356
19–21	0.272 ± 0.012	0.271	0.307	0.447	0.452	1.225	0.679	2.415

the weights, c_k are just the theoretical signal level, using the weights assumes that signal is present in all N_s surfaces. If propagation weighting is applied to a series of surfaces, noise-only points are weighted as if they contained a signal. The probability of noise-only points being weighted strongly enough to be considered signals is highest when the amplitude of the signal is low or when the signal is only present in a small fraction of the surfaces.

To minimize errors in locating the endpoints, the unweighted algorithm should be used for very low track *SNR* and the weighted algorithm for high track *SNR*. From the tables it can be seen that for fixed *SNR* the mean absolute error increases as the propagation standard deviation increases.

5 Application to PACIFIC SHELF 93 data

A series of ocean acoustic experiments referred to as the PACIFIC SHELF trials was completed in September, 1993 by the Defence Research Establishment Pacific, Victoria, B.C., and the Applied Research Laboratory, University of Texas at Austin. The experiment is summarized below and described more fully in Ozard *et al.*[5] The experiments were conducted at a site on the continental slope and shelf regions off Vancouver Island, in the North-East Pacific.

The array float position and tow ship position were measured with Global Positioning System (GPS) receivers. The GPS measurement errors, combined with the tether length

between array and float, resulted in an overall uncertainty of the source-to-receiver range of approximately 200 m.

In Figure 3 the depths of the vertical line array (VLA) used to collect the data are plotted over other environmental information used to model the field. There were sixteen hydrophones equispaced at 15 m with the depth for the uppermost hydrophone being 90 m $\pm$ 2 m. The data were collected at a sample rate of 1500 Hz.

The environmental model was based on the measured sound speed profile, taken at the time of the experiment, and geoacoustic parameters obtained from the analysis of the impulsive source data collected in the vicinity of the array in an associated seismic experiment [5].

The CSS WE RICKER towed the multi-frequency Continuous Wave (CW) towed sound source, while the CFAV ENDEAVOUR collected acoustical data from a VLA. In the portion of the trial analyzed here the CW multi-frequency source was towed at constant speed and heading along two segments that formed a dog leg pattern as shown in Figure 4.

As can be seen the towed source's track began on the continental shelf, where the water depth was about 150 m, and proceeded towards the VLA located in deeper water on the continental slope at an approximate water depth of 375 m. The source tow took a total of about 65 minutes. At the start time, the initial source to receiver range was about 12 km. As can be seen in Figure 4, there was an abrupt source ship course change 41 minutes later.

The measured data for the Bartlett processor is obtained from a 4096 point Fast Fourier Transform of the time series data at the signal frequencies of 45 and 72 Hz or the nearby noise frequencies of 43 or 75 Hz. The source level at 45 Hz was typical of a strong line on a merchant vessel while the 72 Hz line was 20 dB lower. Eleven inner products were averaged; thus each Bartlett output represents about 30 seconds of data. The replica or modeled fields used in the analysis were based on previously described, but limited, environmental knowledge using Westwood's normal mode model, ORCA [6].

Linear tracking algorithms have previously been applied to the ambiguity surfaces produced from this experiment [5]. (The term ambiguity surface will be used even though the surfaces in this case have three dimensions.) Since these algorithms track sources of constant speed and heading the data was partitioned into two sets, before and after the course change, referred to as either A and B or far-range and near-range.

Three dimensional linear tracking, using both weighted and unweighted versions of the algorithm, was done on both the far and near-range data sets for both the 45 Hz and 72 Hz data. For both linear and piecewise tracking, tracks were found by considering all possible tracks connecting one of the top 10 peaks on each surface to one of the top ten peaks on another surface. Duplicate tracks were eliminated by keeping only the highest *SNR* track in the case where two or more tracks start and end coordinates were within 100 metres of each

other. The search region consisted of ranges and bearings forming a 16 km radius quarter circle and depths from 10 to 100 metres.

The top track x-y coordinates obtained with the linear tracking algorithm for each case are shown as a dashed line in Figures 5 to 8. The solid lines represent the tracks found with the piecewise tracker and the dotted line indicates the known track position which has a 200 m uncertainty. All of the tracks in these figures have depths between 17 and 32 metres. As can be seen, there is good agreement in range but less so in bearing. Bearing is determined solely from the environmental symmetry splitting and an extremely small, $\sim 2°$, tilt of the VLA from the vertical. Thus the agreement of the tracks with the known track in range, depth and approximate bearing is convincing evidence for the very significant capability of MFP with tracking

The dashed tracks found with the linear tracker are the best tracks that can be found if the time of the course change is known. For this reason, results obtained with the PTA should be compared to the dashed tracks as opposed to the true dotted track in Figures 5 to 8.

While linear tracking finds tracks through a series of ambiguity surfaces, the application of the PTA enables the identification of the portion of a track with the highest *SNR*. Initially the PTA was applied to the entire set of 130 ambiguity surfaces obtained from the 45 Hz data. The top five piecewise tracks using the unweighted and weighted algorithms, shown in figures 5 and 6 respectively, have a thickness proportional to track *SNR*. In this initial tracking the tracks closest to the array located at the origin of the figures were recovered. With the weighted algorithm, the five tracks with the highest *SNR* succeed in isolating the segment of the true track closer to the array. This is due to the fact that propagation effects in the region cause the track *SNR* to decrease very rapidly as a function of range. This results in the far-range track *SNR* being much less than the near-range track *SNR* and thus the far-range track, although recovered, are not among the top tracks.

To isolate the far-range track without knowing the time of the heading change *a priori*, piecewise tracking was then repeated on only the surfaces not included in the most significant portions of the tracks found by considering all 130 surfaces. The top three tracks using the unweighted algorithm run from surface 94 to surface 130, while the top five obtained with the weighted algorithm run from surface 82 to 130. By repeating piecewise tracking on surfaces 1 to 93 and 1 to 81 it is possible to recover the far-range segment of the track without making any assumptions about when the source changed course. This procedure could then be repeated yet again on the remaining surfaces. The top five tracks in each case are shown in figures 5 and 6, also as solid lines. The start and end coordinates and *SNR* estimates of the tracks in figure 5 are also shown in table 3 and those from figure 6 in table 4.The weighted algorithm gave better performance than the unweighted algorithm as can be seen from figures 5 and 6.

This procedure was then repeated on 129 ambiguity surfaces obtained for the 72 Hz

Table 3: Tracks found using the unweighted PTA on 45 Hz data. The two segments of the true track are shown followed by the highest *SNR* linear tracks for each segment. The next 5 tracks are those found by considering all 130 surfaces followed by 5 found considering only surfaces 1 to 93

Track	X_1	Y_1	Z_1	X_n	Y_n	Z_n	$\widehat{SNR}_u$ (dB)	Surfaces
True A	11243.3	3209.1	30.0	4496.0	592.2	30.0	13.62	1-83
True B	4496.0	592.2	30.0	611.7	920.1	30.0	12.94	83-130
Top A	11628.7	1865.4	20.0	4138.4	1705.1	20.0	15.42	1-83
Top B	4301.9	1223.0	19.8	903.3	742.1	31.5	15.64	83-130
1	2244.6	2948.5	20.0	1273.0	149.6	20.0	18.30	94-130
2	2539.4	2639.3	20.0	1243.5	41.6	20.0	18.26	94-130
3	2005.6	3130.5	20.0	1276.3	171.8	20.0	18.22	94-130
4	4698.5	1710.1	20.0	430.0	1212.4	20.0	17.80	94-130
5	2560.5	5025.3	20.0	1264.2	185.5	20.0	17.65	94-130
1	9984.5	1830.2	20.0	3225.0	1685.5	20.0	15.79	19-93
2	9308.9	2236.2	20.0	3334.4	1477.6	20.0	15.77	24-93
3	9198.0	2518.3	20.0	3389.9	1336.6	20.0	15.77	24-93
4	9419.6	1977.3	20.0	3279.1	1607.1	20.0	15.76	24-93
5	9897.0	2072.6	20.0	3169.0	1809.1	20.0	15.76	19-93

data (the first 30 second surface was omitted). In this case the top five tracks found by applying the unweighted algorthm to all 129 surfaces run from surface 66 to 130 and four of the top five tracks found with the weighted algorithm run from surface 79 to 124. Second runs were then conducted on surfaces 2 to 65 and 2 to 78 respectively. The 72 Hz results are shown in figures 7 and 8 and tables 5 and 6. Again the weighted algorithm gave better performance than the unweighted algorithm.

6 Conclusion

In real world applications of tracking algorithms, start and stop times of linear or circular track segments would be unknown. This paper described a piecewise tracking algorithm (PTA) which does not assume the above quantities are known *a priori*. For the idealized case of constant signal, known except for phase and spatially white noise, a series of simulations shows that start and stop times can be determined with mean absolute error equal to the time covered by 3 or fewer surfaces if the track *SNR* is greater than 13. The PTA was then applied to previously-analyzed data from the PACIFIC SHELF trial where the source changes heading. The weighted form of the PTA was able to identify the change of heading and almost exactly reproduce results obtained by the linear tracking algorithm which requires the change of heading time to be known *a priori*. In the case studied here

Table 4: Tracks found using the weighted PTA on 45 Hz data. The two segments of the true track are shown followed by the highest SNR linear tracks for each segment. The next 5 tracks are those found by considering all 130 surfaces followed by 5 found considering only surfaces 1 to 81

Track	X_1	Y_1	Z_1	X_n	Y_n	Z_n	$\widehat{SNR}_w$ (dB)	Surfaces
True A	11243.3	3209.1	30.0	4496.0	592.2	30.0	14.31	1-83
True B	4496.0	592.2	30.0	611.7	920.1	30.0	13.52	83-130
Top A	11628.7	1865.4	20.0	4138.4	1705.1	20.0	15.92	1-83
Top B	4301.9	1223.0	19.8	903.3	742.1	31.5	16.28	83-130
1	4480.8	1002.8	20.0	769.8	907.1	20.0	18.96	82-130
2	4337.5	1391.6	20.0	654.0	1044.3	20.0	18.96	82-130
3	4119.1	1718.8	20.0	697.7	978.9	20.0	18.96	82-130
4	4360.8	1333.2	20.0	649.3	1056.0	20.0	18.96	82-130
5	4397.5	1119.2	20.0	791.7	876.5	20.0	18.95	82-130
1	11488.1	1885.9	34.9	4537.4	1749.9	17.8	15.55	2-79
2	11582.0	1752.0	20.0	4964.5	1942.8	20.0	15.55	2-73
3	11082.8	2778.9	20.0	5046.3	1774.4	20.0	15.54	2-73
4	11248.2	2373.1	20.0	5019.2	1840.9	20.0	15.54	2-73
5	11442.6	2133.1	20.0	4987.4	1880.3	20.0	15.54	2-73

Table 5: Tracks found using the unweighted PTA on 72 Hz data. The two segments of the true track are shown followed by the highest SNR linear tracks for each segment. The next 5 tracks are those found by considering all 130 surfaces followed by 5 found considering only surfaces 2 to 65

Track	X_1	Y_1	Z_1	X_n	Y_n	Z_n	$\widehat{SNR}_u$ (dB)	Surfaces
True A	11161.0	3177.2	30.0	4496.0	592.2	30.0	11.34	1-83
True B	4496.0	592.2	30.0	611.7	920.1	30.0	11.23	83-130
Top A	10049.0	4474.1	20.0	4129.2	1838.4	20.0	15.65	1-83
Top B	4772.4	183.4	20.0	896.4	844.8	20.0	15.67	83-130
1	6214.1	636.6	20.0	592.7	1100.4	20.0	17.21	65-130
2	6037.4	1101.0	20.0	534.0	1192.3	20.0	17.15	65-130
3	6264.6	538.6	20.0	635.4	1042.8	20.0	17.13	65-130
4	6007.6	1167.8	20.0	555.7	1143.6	20.0	17.12	65-130
5	6171.1	800.9	20.0	598.0	1080.3	20.0	17.09	65-130
1	8530.1	3446.4	20.0	5934.0	2397.5	20.0	15.04	25-60
2	8774.4	3021.3	20.0	6127.0	2109.7	20.0	15.02	25-60
3	8368.1	3725.7	20.0	5810.1	2586.8	20.0	15.02	25-60
4	8682.8	3160.3	20.0	6051.6	2202.6	20.0	15.00	25-60
5	8468.6	3594.7	20.0	5891.2	2500.7	20.0	14.96	25-60

Table 6: Tracks found using the weighted PTA on 72 Hz data. The two segments of the true track are shown followed by the highest *SNR* linear tracks for each segment. The next 5 tracks are those found by considering all 130 surfaces followed by 5 found considering only surfaces 2 to 78

Track	X_1	Y_1	Z_1	X_n	Y_n	Z_n	$\widehat{SNR}_w$ (dB)	Surfaces
True A	11161.0	3177.2	30.0	4496.0	592.2	30.0	11.97	1-83
True B	4496.0	592.2	30.0	611.7	920.1	30.0	12.26	83-130
Top A	10049.0	4474.1	20.0	4129.2	1838.4	20.0	16.17	1-83
Top B	4749.1	376.0	19.5	833.6	962.0	30.2	15.86	83-130
1	6870.6	360.1	30.0	1597.8	83.7	30.0	18.24	58-124
2	4803.5	991.4	20.0	1417.2	715.1	20.0	18.14	79-124
3	4796.0	965.2	20.0	1423.2	736.1	20.0	18.13	79-124
4	4883.7	817.1	20.0	1353.1	854.6	20.0	18.13	79-124
5	4882.8	780.3	20.0	1353.7	884.0	20.0	18.12	79-124
1	9537.4	4246.3	20.0	4494.6	2001.1	20.0	16.01	9-78
2	9461.9	4412.1	20.0	4531.5	2113.1	20.0	15.96	9-77
3	9642.7	3895.9	20.0	4673.0	1888.0	20.0	15.95	10-77
4	9266.5	4721.5	20.0	4348.1	2215.5	20.0	15.95	9-78
5	9610.1	4079.2	20.0	4528.9	1922.4	20.0	15.92	9-78

propagation loss changed quickly as a function of range and significant tracks were found on only some of the ambiguity surfaces. The PTA, when run with these surfaces omitted, recovered the significant tracks on the remaining surfaces.

References

[1] A. Tolstoy, *Matched-field processing for underwater acoustics*, (World Scientific, Singapore, 1993).

[2] M. Musil, J.M. Ozard and M.J. Wilmut, "Efficient Matched Field Tracking Algorithms," Defence Research Establishment Atlantic, Technical Memorandum 97- (1997).

[3] M.J. Wilmut, J.M. Ozard and P. Brouwer, "Evaluation of two efficient target tracking algorithms for matched-field processing with horizontal arrays," *J. of Computational Acoustics* **3**,(1995) 311-326.

[4] M.J. Wilmut, J.M. Ozard and B. Woods, "An efficient target tracking algorithm for matched field processing," IEEE *Oceans 93*, 19-22-October 1993, Victoria, B.C. Canada, **III**, (1993) 86-90.

[5] J.M. Ozard, M.L. Yeremy, N.R. Chapman and M.J. Wilmut, "Matched-field processing in a strongly range-dependent shallow water environment in the north-east Pacific Ocean," *IEEE, J. Oceanic Eng.*, **21**, (1996) 377-383.

[6] E.K. Westwood, C.T. Tindle and N.R. Chapman, "A normal mode model for acoustic-elastic ocean environments," *J. Acoust. Soc. Am.*, **100**, (1996) 3631-3645.

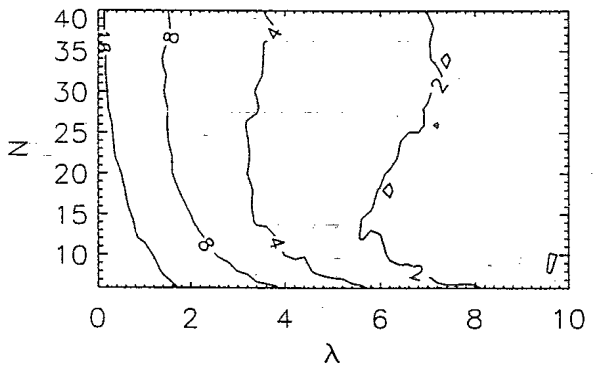

Figure 1: Mean absolute error as a function of signal height, λ, and signal width, N, using the unweighted algorithm with propagation standard deviation $\sigma_w = 0.8$.

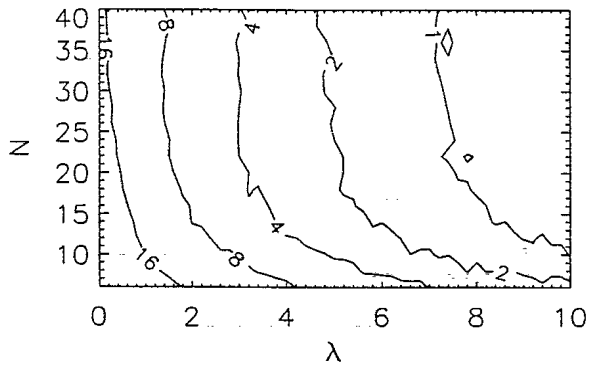

Figure 2: Mean absolute error as a function of signal height, λ, and signal width, N, using the weighted algorithm with propagation standard deviation $\sigma_w = 0.8$.

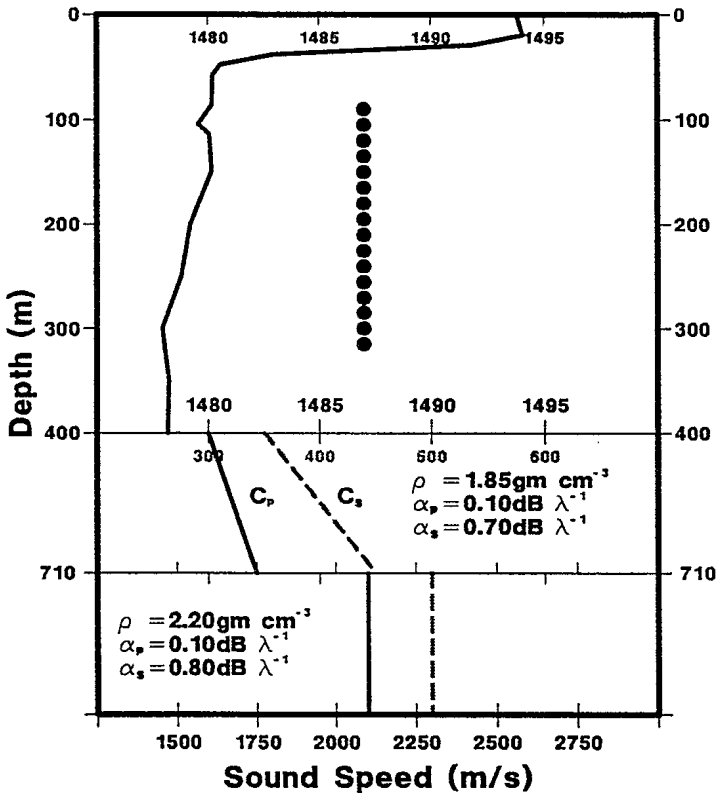

Figure 3: The sound-speed profile used in the environment model is shown as well as the shear speed (dashed) and compressional speed (solid) for which the two lower abscissa scales apply respectively. The hydrophone depths are also noted.

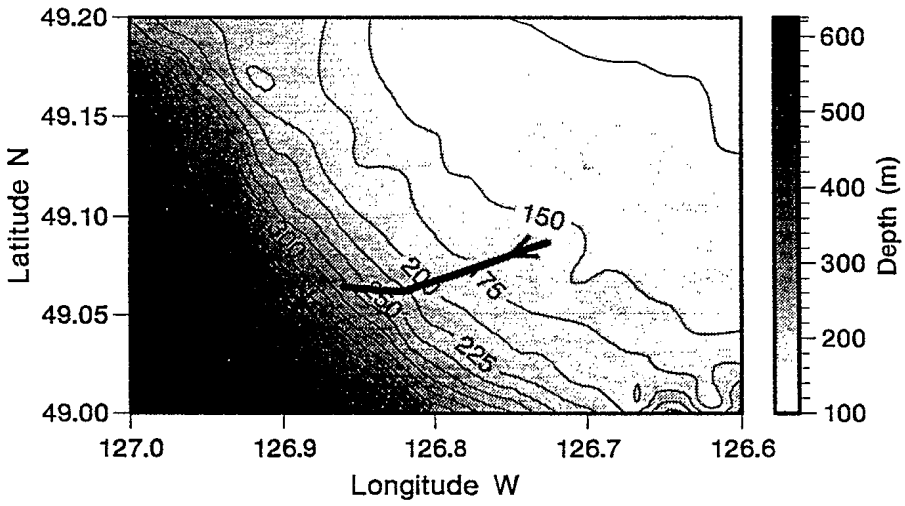

Figure 4: The bathymetry of the region of the PACIFIC SHELF experiment. The line represents the track of the towed source with the tow direction shown by the arrow. The star shows the location of the VLA.

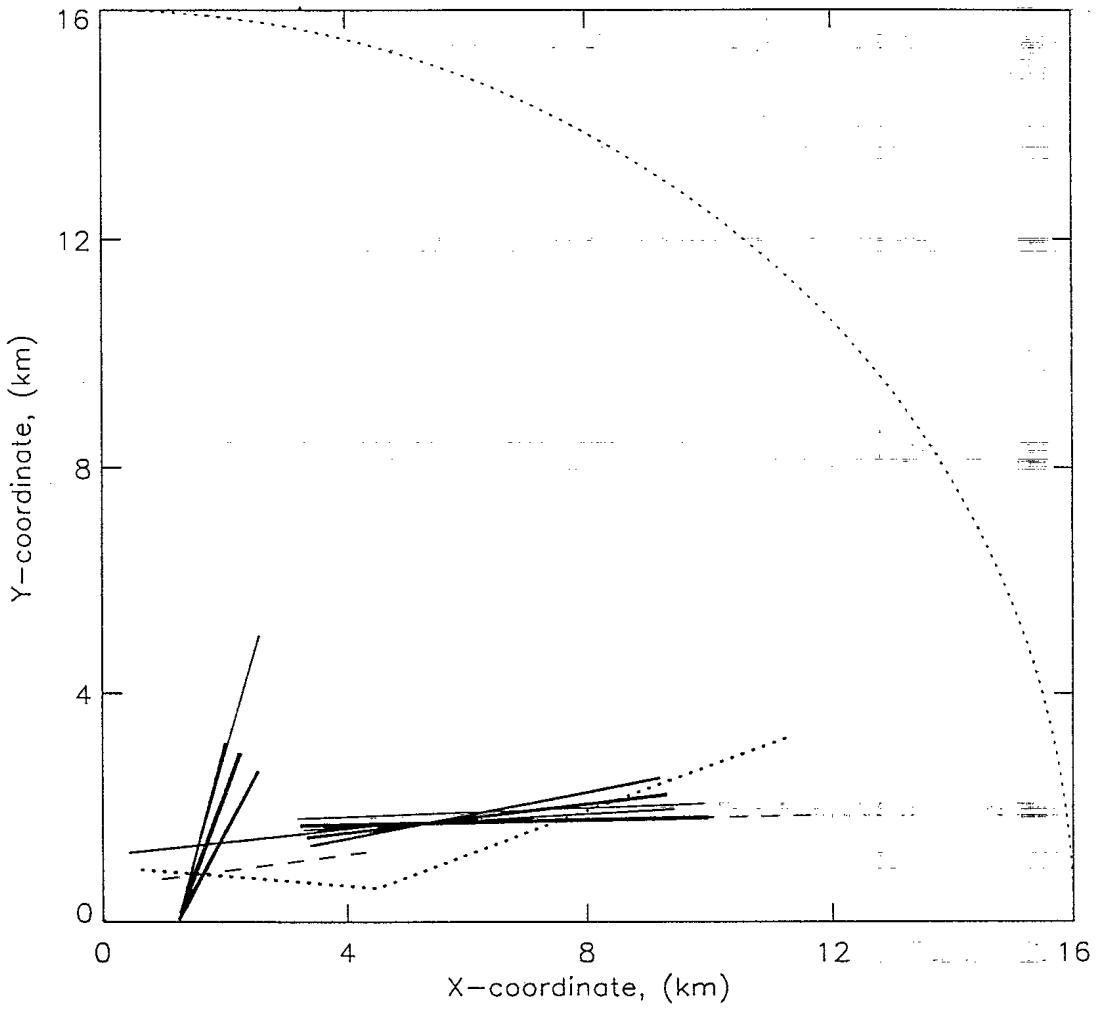

Figure 5: Tracks located using the unweighted piecewise tracking algorithm on the 45 Hz data. The shorter solid lines near the origin are the top 5 tracks found by considering all 130 surfaces. Decreasing line thickness corresponds to decreasing *SNR*. The longer solid lines furthest from the origin are the top tracks found in surfaces 1 to 93. The true track is shown with the dotted line. The dashed lines are the top tracks found by considering sections A and B separately and the dotted quarter circle is the limit of the search area. The tracks are all at depths from 19 to 32 m as shown in Table 3.

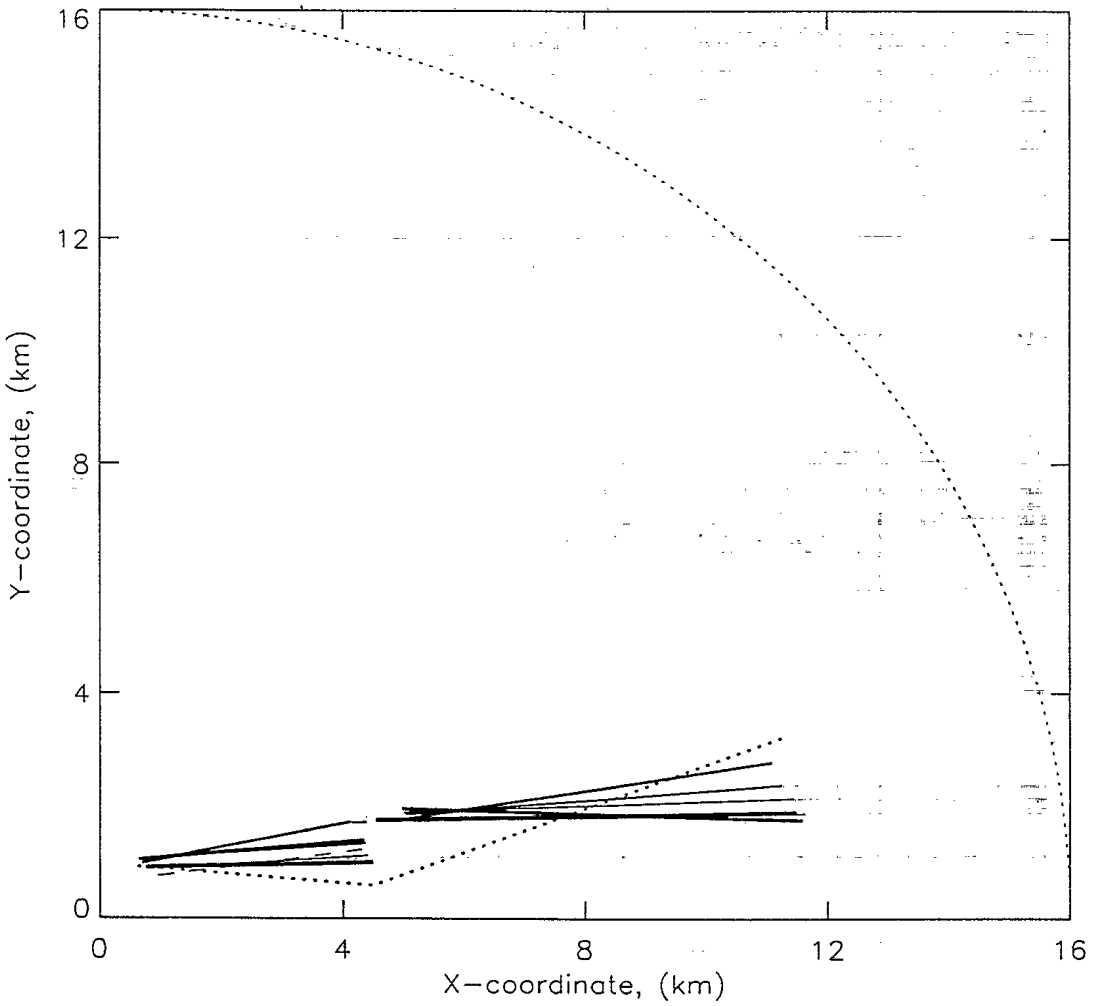

Figure 6: Tracks located using the weighted piecewise tracking algorithm on the 45 Hz data. The shorter solid lines near the origin are the top 5 tracks found by considering all 130 surfaces. Decreasing line thickness corresponds to decreasing *SNR*. The longer solid lines furthest from the origin are the top tracks found in surfaces 1 to 81. The true track is shown with the dotted line. The dashed lines are the top tracks found by considering sections A and B separately and the dotted quarter circle is the limit of the search area. The tracks are all at depths from 17 to 32 m as shown in Table 4.

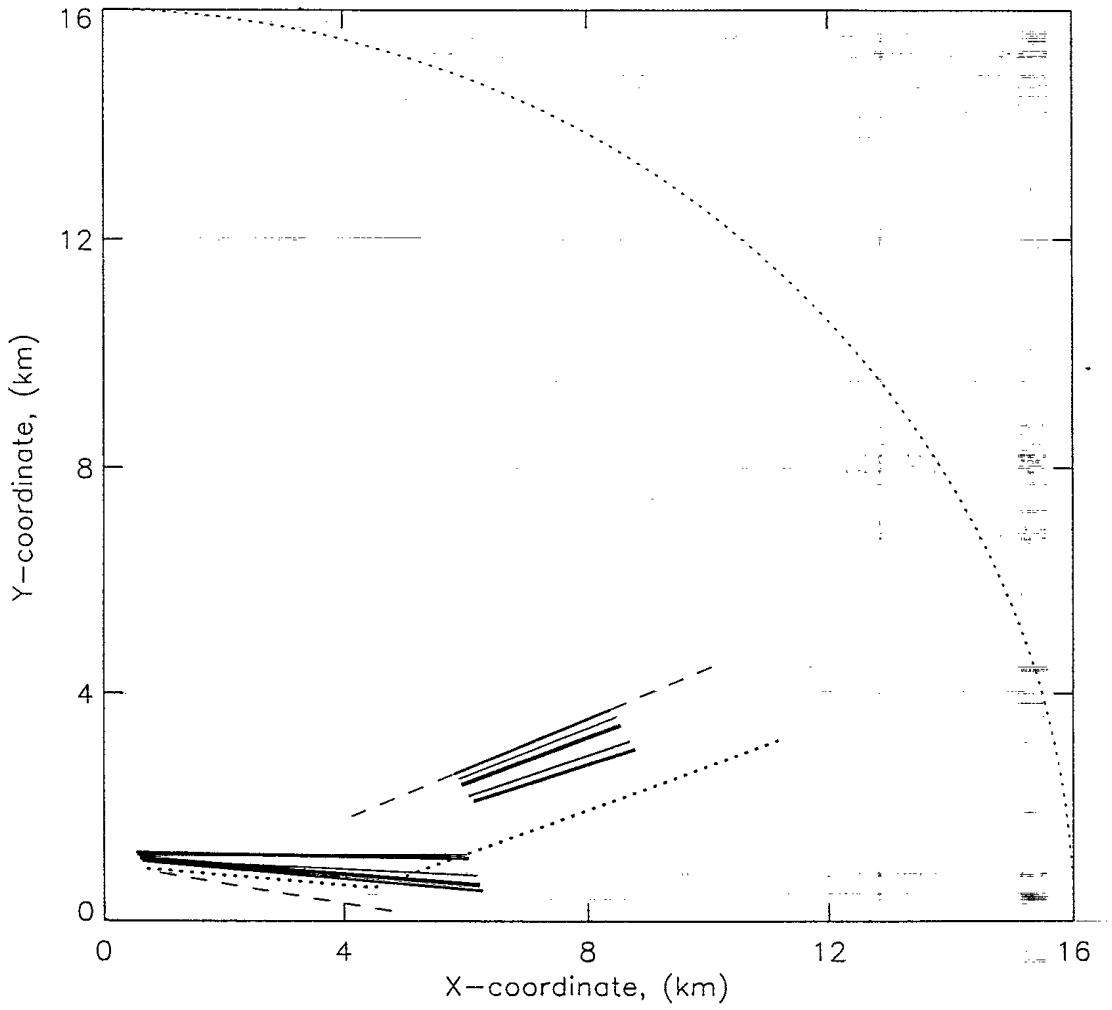

Figure 7: Tracks located using the unweighted piecewise tracking algorithm on the 72 Hz data. The solid lines near the origin are the top 5 tracks found by considering all 129 surfaces. Decreasing line thickness corresponds to decreasing *SNR*. The solid lines furthest from the origin are the top tracks found in surfaces 2 to 65. The true track is shown with the dotted line. The dashed lines are the top tracks found by considering sections A and B separately and the dotted quarter circle is the limit of the search area. The tracks are all at a depth of 20 m as shown in Table 5.

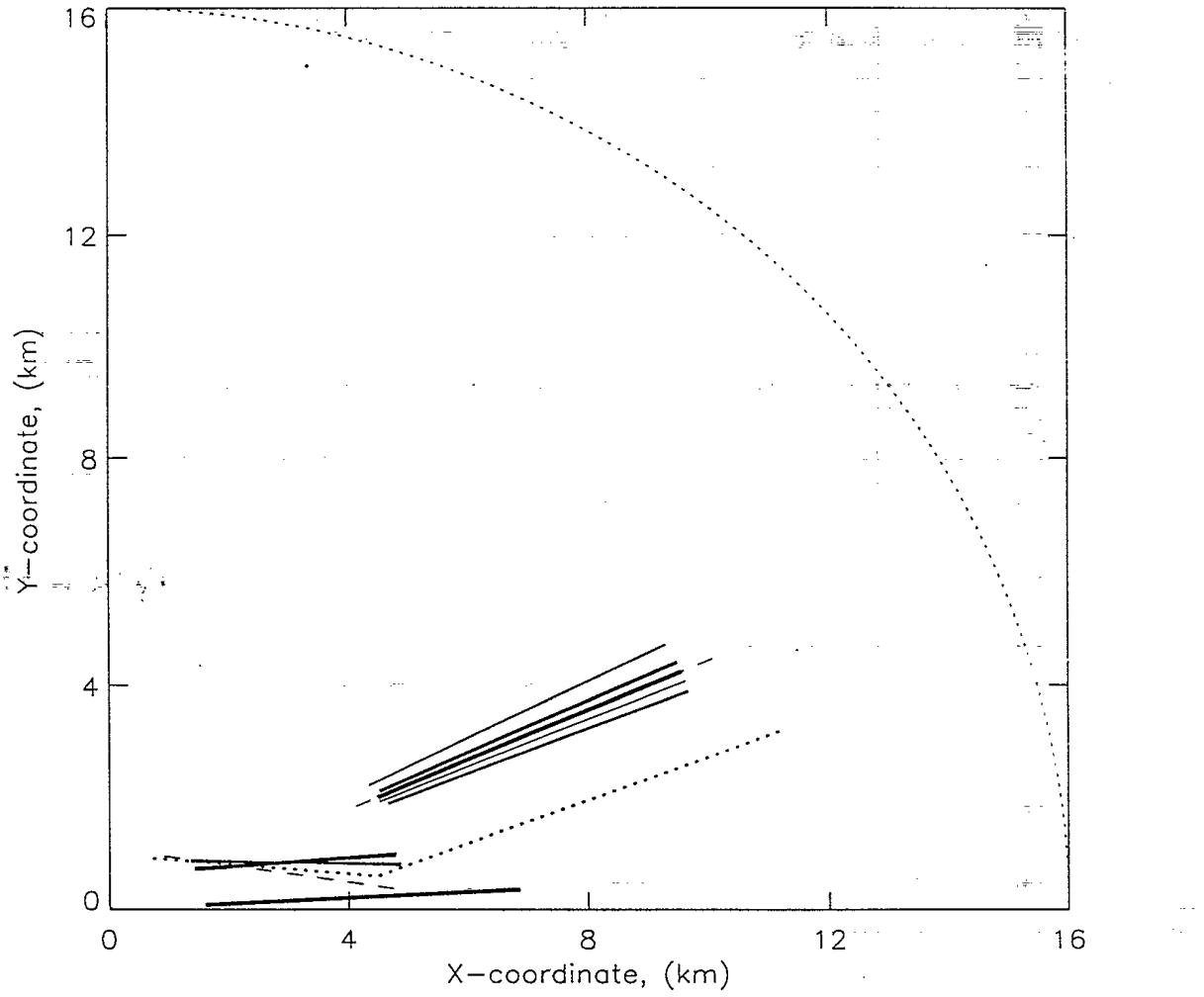

Figure 8: Tracks located using the weighted piecewise tracking algorithm on the 72 Hz data. The shorter solid lines near the origin are the top 5 tracks found by considering all 129 surfaces. Decreasing line thickness corresponds to decreasing *SNR*. The longer solid lines are the top tracks found in surfaces 2 to 79. The true track is shown with the dotted line. The dashed lines are the top tracks found by considering sections A and B separately and the dotted quarter circle is the limit of the search area. The tracks are all at depths from 19 to 32 m as shown in Table 6.

#506552

98-00047